PERGAMON

International Journal of Heat and Mass Transfer 45 (2002) 3131–3142

International Journal of HEAT and MASS TRANSFER

www.elsevier.com/locate/ijhmt

High performance miniature heat pipe ☆

Lanchao Lin [a,*], Rengasamy Ponnappan [b], John Leland [b,1]

[a] UES, Inc., 4401 Dayton-Xenia Road, Dayton, OH 45432-1894, USA

[b] Propulsion Directorate, Air Force Research Laboratory, Wright-Patterson AFB, OH 45433-7251, USA

Received 10 May 2001; received in revised form 8 January 2002

Abstract

High performance miniature heat pipes are developed for the cooling of high heat flux electronics using new capillary structures made of a folded copper sheet fin. Using the folded sheet fin, capillary flow channels with fully and partially opened grooves are made by electric-discharge-machining technique. It is easy to form the capillary grooves as dense as desired through the present fabrication techniques. Heat pipes with two different capillary structures and different fill amounts are tested in the horizontal orientation. Three heating modes of the evaporator are simulated by activating different numbers of chip resistors. The heat pipe with partially opened groove wick performs better than that with fully opened groove wick. The condenser heat transfer coefficient is higher by 120% or greater in the case of the former wick type compared to the latter at an operating temperature of 110 °C. Heat fluxes higher than 140 W/cm^2 are achieved using concentrated heating modes.

1. Introduction

Advanced packages of high power electronics for the US Air Force and space related programs require the use of high performance heat transfer devices to remove high heat flux heat from the power electronics. Heat fluxes higher than 100 W/cm^2 are current projected levels for the advanced power electronics whereas the upper limit of the operating temperature of the power electronics is set below 120 °C [1]. Passive cooling methods using heat pipes have garnered attention due to continuous development in heat pipe theory and application [2–4]. Miniature heat pipe (MHP) is one of the promising heat transfer devices capable of dealing with the high heat flux electronics cooling.

Plesch et al. [5] reported their test results of two different 7 mm wide, 2 mm thick and 120 mm long MHPs. It was found that the heat pipe with longitudinal grooves had a greater heat transport rate. The maximum heat flux was 35 W/cm^2 and the temperature drop over the heat pipe in this case was about 35 °C in the horizontal orientation. Cao et al. tested two MHPs with axial grooves [6]. The heat pipe shell as well as the grooves were fabricated using electric-discharge-machining (EDM) technology. The depth, width and pitch of the groove for one of their heat pipes were 0.25 mm, 0.1 mm and 0.2 mm. The overall dimensions for the heat pipe were 7 mm wide, 2mm thick and 80 mm long. The maximum heat input and evaporator heat flux were about 31 W and 20.6 W/cm^2 for the horizontal arrangement. More recently, Faghri and Khrustalev [7] reported that their copper-water MHP with axial rectangular microcapillary grooves could remove heat at heat flux levels of 82 W/cm^2 from a heating area of 1.4 cm^2 and 150 W/cm^2 from a heating area of 0.7 cm^2 in the horizontal orientation at an operating temperature of 90 °C. To provide a simple and low cost solution to the manufacturing of microwick structures, Ponnappan [8] investigated a new folded-screen wick, copper-water MHP. It was indicated that on a small heating area of 0.774 cm^2, the MHP of this type could handle a heat flux of 115 W/cm^2 at an operating temperature of

☆ This paper is declared a work of the US Government and is not subject to copyright protection in the United States.

* Corresponding author. Tel.: +1-937-255-2922; fax: +1-937-904-7114.

E-mail address: lanchao.lin@afrl.af.mil (L. Lin).

[1] Presently with University of Dayton Research Institute.

0017-9310/02/$ - see front matter
PII: S0017-9310(02)00038-8

Nomenclature

A_h	heating area (m^2)
A_c	cooling area (m^2)
A_1	heating area of one chip resistor (m^2)
B	inner cross-section width (m)
B_f	width of wick structure (m)
h_c	condenser heat transfer coefficient (W/m^2 K)
h_e	evaporator heat transfer coefficient (W/m^2 K)
k	thermal conductivity (W/m K)
L	length (m)
n_h	number of active chip resistor heater
q_e	evaporator heat flux (W/m^2)
Q	total heat rate (W)
Q_{bot}	heat rate through bottom cooler (W)
Q_{loss}	heat losses (W)
Q_{top}	heat rate through top cooler (W)
t_w	heat pipe wall thickness (m)
T_v	heat pipe operating temperature (°C)
ΔT_{ec}	average evaporator-to-condenser temperature difference (°C)

Subscripts

a	adiabatic
c	condenser
e	evaporator
i	inner
m	mean

90 °C and evaporator-to-adiabatic temperature difference of 37 °C [8]. By comparison of the published results of MHPs [5–8], the MHP with microcapillary grooves (0.2 mm wide by 0.42 mm deep) [7] was superior in the heat transfer characteristics. In spite of the high performance, the evaporator-to-condenser temperature difference of the MHP with microcapillary grooves reached 21 °C at 100 W or 64 W/cm^2 in the evaporator and this indicates that at the high heat flux, the heat pipe internal thermal resistance was high.

To decrease the internal thermal resistance of MHP at high evaporator heat fluxes, Researchers at the Air Force Research Laboratory (AFRL) have developed high performance MHPs which contain new capillary structures made of a folded copper sheet fin. Particularly, a heat transfer enhancement method is developed that deals with a notched folded sheet fin. The notches appear only in the evaporator and condenser. The fins are brazed onto either wide side of the MHP. The notches (small slits) let the vapor escape from the groove into the vapor core. As opposed to the notches, the fin bridges (uncut part at the fin top) separating notches at the top of the fin protect the returning liquid against the interfacial shear stress of countercurrent two-phase flow to some extent and consequently reduce the liquid flow resistance. Meanwhile, the fin bridges in the condenser serve as additional secondary heat transfer area and contribute to the enhancement of condensation heat transfer. For closed two-phase thermosyphons, the reduction of the interaction between the vapor and liquid flows was achieved using a perforated tube flow separator [9]. For the present MHP, the notched fin functions as two-phase flow separator. The objective of the present study is to compare thermal performances of the heat pipes with new capillary structures and to verify the heat transfer enhancement method, especially under high heat fluxes.

2. Design of miniature heat pipes

The MHPs developed at AFRL have more flexible capillary structures compared to the machined wicks reported [5–7]. One basic configuration is a heat pipe with capillary fins on its inner wall. One half-section of the MHP fin wick assembly is shown in Fig. 1. The fin wick assembly is made by brazing a folded sheet on the wide side and making a full cut on the top of the fins using EDM technology. Like conventional heat pipes, the operation of a MHP is subject to performance limitations. The type of performance limitation that restricts the operation of a MHP is determined by computing which limitation has the lowest value at a given heat pipe operating temperature. Some performance limitations of heat pipe depend on types of capillary structures. One of the most commonly used capillary structures is formed by axial grooves. It may be noted that the present capillary fin wick heat pipe is analogous to the traditional axially grooved heat pipe.

To enhance the capillary pressure, the groove width must be small. However, to decrease the liquid pressure drop in the wick, the groove width must be large. In most cases, the heat flux travels radially through the

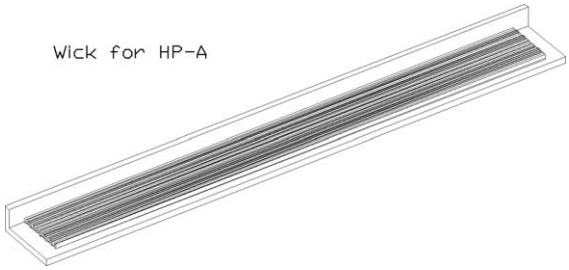

Fig. 1. Capillary fins (fully opened grooves).

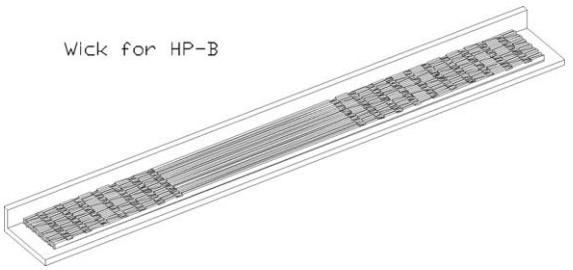

Fig. 2. Folded sheet fin (partially opened grooves) with notches cut at its top in the evaporator and condenser.

capillary structure to evaporate the working fluid. For a small radial temperature drop through the capillary structure, the saturated capillary structure must be thin in the radial direction and have a high thermal conductivity. This consideration usually results in a small cross-sectional area of the liquid flow, which conflicts with the need for a small liquid pressure drop from the condenser to the evaporator.

The performance of the axially grooved heat pipe could be improved by decreasing the groove width and pitch and increasing the groove depth to some extent. This approach is more effective at low operating temperatures, e.g., less than 100 °C for the water heat pipe. Considering a constraint of machining cost, a 0.13 mm wide by 0.64 mm deep groove is probably the narrowest and deepest dimension that can be made in aluminum [10]. To reduce the ratio of the groove width to groove depth further, AFRL researchers have developed the heat pipe with the capillary fins as shown in Fig. 1. Since it is easy to make a very small groove width between two consecutive fins of a folded sheet, a high pumping ability of the capillary fin is achievable at low fabrication cost.

To further enhance the maximum performance and thermal performance of the heat pipe, AFRL researchers have developed an enhanced folded copper sheet fin structure with notches cut at the top of the fin in the evaporator and condenser. Fig. 2 shows this type of the fin. The fin bridges (uncut part) separating notches on the top of the fin protect the return liquid against the interfacial shear stress of countercurrent two-phase flow to some extent. Meanwhile, the cut holes let the vapor escape from the groove into the vapor core. The uncut part of the folded fin in the heat pipe condenser serves as additional secondary heat transfer area enhancing condensation heat transfer.

3. MHP fabrication details

The heat pipe with the fully opened capillary fins and that with the partially opened folded fin are denoted as HP-A and HP-B, respectively. The dimensions of the capillary fin and the cross-sectional view of HP-A are shown in Fig. 3. For HP-B, the similar folded sheet fin is used but notch cuts at the top of the fin are made instead of the full cut. The dimensions of the folded sheet fin with notch cuts are shown in Fig. 4. The notch cuts are evenly distributed along the heat pipe length and made only in the evaporator and condenser sections. The geometric parameters of the fin assemblies for HP-A and HP-B are included in Table 1. Two similar assemblies are required to build a heat pipe. In Table 1, the inner cross-section refers to the cross-sectional area bounded by the inner wall and the outer cross-section to the heat pipe outer wall. The evaporator length is related with three chip resistors on each side. The notch pitch is set constant along the heat pipe length. The brazing temperature for the assembly of heat pipe parts is 655 °C.

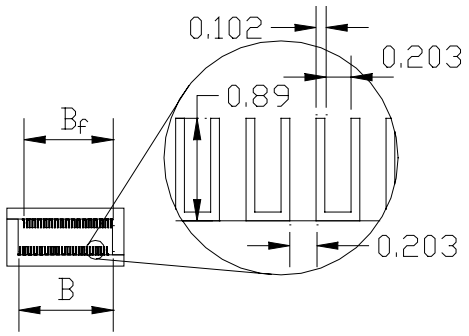

Fig. 3. Dimensions of capillary fins (in mm).

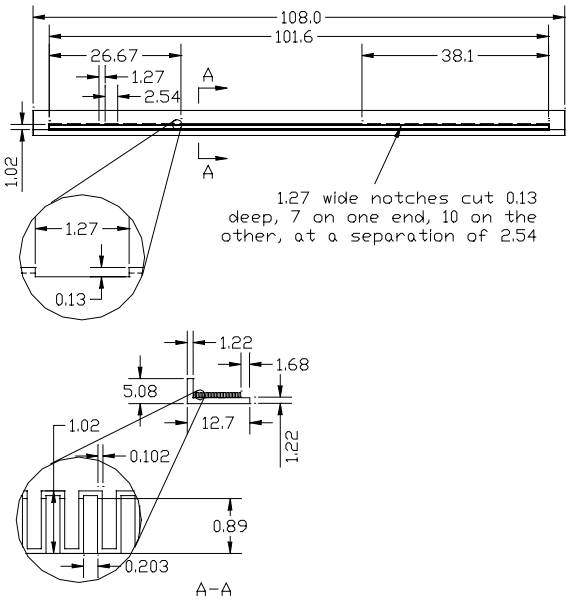

Fig. 4. Dimensions of notched folded sheet fin (in mm).

Table 1
Design features and dimensions of wick assemblies for HP-A and HP-B

Parameters	HP-A	HP-B
Total MHP length (mm)	108	108
Inner cross-section (mm^2)	10.26(B) × 3.91	10.26(B) × 3.91
Outer cross-section (mm^2)	12.7 × 6.35	12.7 × 6.35
L_e((6 chips)/L_a/L_c) (mm)	18.5/50.6/32.5	18.5/50.6/32.5
Notch number in L_e/L_c	Full cut	7/10
Fin length/width (mm)	101.6/9.76(B_f)	101.6/9.76(B_f)
Fin height (mm)	0.89	1.02/0.89(cut)
Fin thickness (mm)	0.1	0.1
Fin pitch (mm)	0.305	0.305
Fin number (one side)	32	32
Notch width/depth (mm)	–	1.27/0.13
Notch pitch (mm)	–	3.81

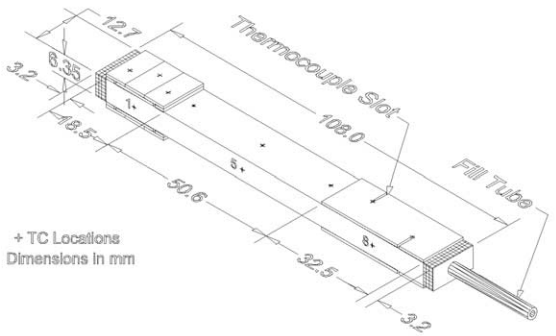

Fig. 5. Heat pipe assembly and its dimensions.

Fig. 5 shows a typical heat pipe assembly and its overall dimensions. The assembly includes two copper angles holding the capillary fins, two end caps, and one copper tube for the filling of working fluid. The brazing material is used at the junctions of the parts.

The brazed assembly of the heat pipes are baked at 150 °C, evacuated to a pressure of 3×10^{-6} Torr for 24 h, and filled with distilled water. After the filling, the copper tube is pinched and welded. The working fluid fill amounts, measured at 25 °C, are 1.3 and 0.87 ml for HP-A and 1.3 and 0.85 ml for HP-B. A ratio of the working fluid fill amount to the volume of all the grooves is referred to as fill ratio. The 0.87 ml fill amount for HP-A corresponds to a fill ratio of 80% and the 0.85 ml fill amount for HP-B corresponds to a fill ratio of 78%.

4. Experimental setup and procedure

Six chip resistors are mounted onto the wide side wall to simulate the heat source of electronic components, three on the top and three on the bottom of the heat pipe. Fig. 6 shows three different heating modes indicated by active chip resistors. Each chip resistor, with 12.55 mm long and 6.17 mm wide, has a contact heating area of $A_1 = 0.774$ cm^2, and the shorter side is marked in black as shown in Fig. 6. Mode 1 heater has only one active chip resistor at the bottom. Mode 2 heater consists of two active chip resistors in the middle. In mode 3 heater, all chip resistors are switched on.

Thermocouple locations on the heat pipe are shown in Fig. 7. There are eight thermocouples at the top surface, and eight at the bottom surface in the symmetric positions in reference to the thermocouples above. Three

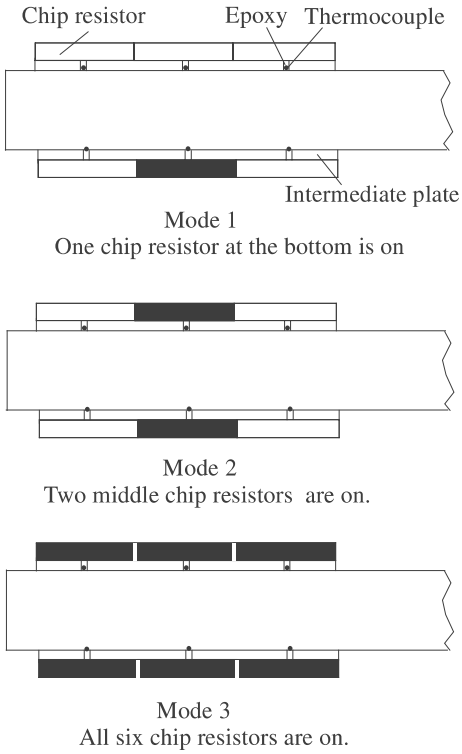

Fig. 6. Evaporator heating modes.

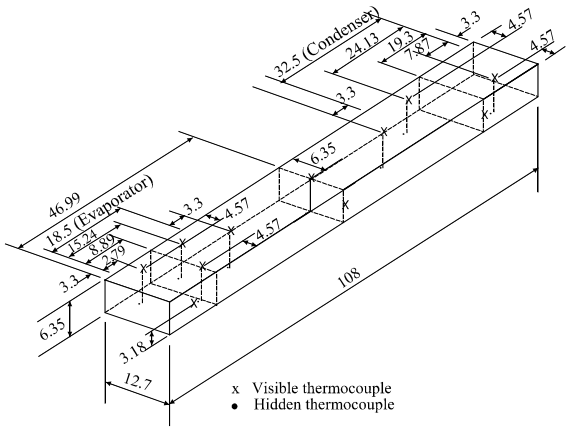

Fig. 7. Thermocouple locations.

thermocouples are placed on the side-wall of the MHP. Two intermediate plates with three slots are soldered onto the evaporator and another two plates with two slots are soldered onto the condenser to protect the thermocouples against a contact with the heater or cooler. The thickness of the intermediate plate is 0.8 mm. Six thermocouples in the evaporator and four thermocouples in the condenser are inserted into the thermocouple slots and soldered onto the heat pipe wall. The slot width is 0.51 mm and is sized to accommodate the thermocouple wire of 0.08 mm in diameter and 0.3 mm in bead diameter. Epoxy is filled in the thermocouple slots to insulate the thermocouple from the chip heater and from the cooler. The chip resistors are soldered onto the top and bottom intermediate plates in the evaporator, making the intermediate plate sandwiched between the chip resistor and the heat pipe. Two coolers are clamped onto the top and bottom intermediate plates in the condenser.

The schematic of a MHP experimental setup is shown in Fig. 8. A DC power supply unit is used to provide DC power for the heaters. The chip resistors are built in parallel and connected with switches so that the chip resistors can selectively be turned on and off to arrange different heating modes. Two coolers are employed in the heat pipe condenser. Inside the cooler, there is a rectangular channel with plain fins mounted on its contact side with the condenser. Two turbine flow meters are used to measure the coolant flow rates through the top and bottom coolers. The turbine flow meter is operated with a signal conditioner. The coolant flow rates are regulated by two valves in the upper and lower flow channels. The flow rates through the top and bottom coolers are set to be approximately equal. The coolant temperatures at the inlet and outlet of the coolers are measured using two type T probe thermocouples. The coolant temperature is regulated by a constant temperature bath (cold bath) with 500 W capacity. A pressure transducer is installed at the coolant channel to measure the coolant supply pressure that is partially controlled by a bypass valve. The coolant flow circulation is maintained by a water pump.

The operating temperature of the heat pipe, T_v, is monitored by the thermocouple in the middle of the adiabatic section. The operating temperature is adjusted by regulating the coolant flow rate and the cold bath temperature. The experimental parameters are listed as follows:

Operating temperature	60, 80, 90, 100, 110 °C
Input power (W)	10–250 W
MHP orientation	Horizontal operation

The actual total heat rate through the heat pipe is estimated by subtracting heat losses, Q_{loss}, from the input power. To measure the heat loss at various specific heat pipe operating temperatures, a small electric power

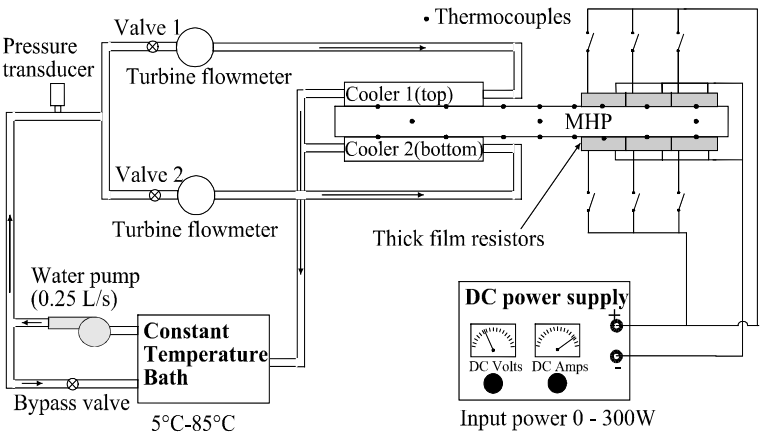

Fig. 8. Schematic of MHP experimental setup.

load is applied to the chip resistor on the heat pipe with coolers removed. The whole heat pipe is insulated. The value of the applied electric power load is adjusted until a specific operating temperature is reached. As a result, the heat losses of 1.2, 2.15 and 2.90 W were measured at the operating temperatures of 60, 90 and 110 °C. With the tested heat losses at various operating temperatures, the actual total heat rate is obtained as follows:

$$Q = IV - Q_{\text{loss}}, \tag{1}$$

where I is the total electric current through the heaters on the heat pipe and V is the voltage across the heaters.

For heat transfer analysis, average temperatures in the evaporator, condenser and adiabatic section are calculated. The average evaporator temperature is an arithmetic average on temperatures indicated by the thermocouples covered with the active chip resistors. For mode 1, mode 2 and mode 3 heating configurations, the average temperature respectively involves one thermocouple, two thermocouples and six thermocouples. The average adiabatic temperature involves two thermocouples on the middle top and bottom surfaces of the adiabatic section. The average condenser temperature involves four thermocouples on the top and bottom surfaces of the condenser.

5. Measurement uncertainty

The Hewlett Packard 3852A data acquisition system is used to make all temperature measurements. This device has a resolution of 0.02 °C. The data acquisition unit and type T thermocouples (19 0.08 mm diameter thermocouples and four probe type thermocouples) are compared to a precision digital RTD with 0.03 °C rated accuracy over the range of interest and the system accuracy is found to be within 0.1 °C. In the steady state, the wall thermocouples fluctuate within 0.2 °C. The accuracy of the thermocouple locations is within 0.5 mm in the heat pipe axial direction.

The actual total heat rate (Q) through the heat pipe is estimated based on the measurement of heat losses of the insulated heat pipe with coolers removed. The DC power applied to the heat pipe is supplied by the Hewlett Packard 6030A System Power Supply unit. The accuracy of the voltage is 0.035% + 145 mV and the accuracy of the current is 0.02% + 25 mA. The overall uncertainty of the heat rate through the heat pipe is predicted using the standard Kline and McClintock approach to the calculation of random uncertainty [11]. The same approach is taken for the calculation of other overall uncertainties hereafter. For HP-A with 0.87 ml fill amount, the predicted overall uncertainty of the heat rate is shown in Fig. 9. The uncertainty of Q varied from 5.7% at 10 W input power to 0.8% at 210 W input power. The uncertainty of Q for other MHPs varies only slightly compared to the case of HP-A.

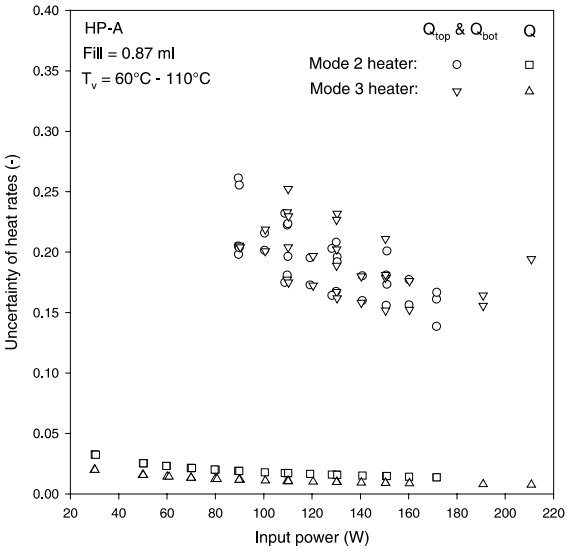

Fig. 9. Uncertainties of the total heat rate through HP-A, the heat rate through the top condenser (Q_{top}) and the bottom condenser (Q_{bot}) vs. the input power.

To compare the heat rate through the top cooler (Q_{top}) and bottom cooler (Q_{bot}) at heat rates higher than 90 W, calorimetry is applied by measuring the flow rate of the coolant and the coolant temperatures at the inlet and outlet of the coolers. Two turbine flow meters (OMEGA FP-541 flow sensor) working with signal conditioners are used to measure the coolant flow rate. The turbine flow meters are calibrated for water. The uncertainty of the turbine flow meter is 0.5% of full scale. The uncertainties of Q_{top} and Q_{bot} are predicted for various operating conditions. Typically, the results for HP-A are also shown in Fig. 9. The results are associated with mode 2 and mode 3 heaters and with the operating temperatures of 60–110 °C. It is indicated that the uncertainties of Q_{top} and Q_{bot} decrease with an increase in the input power and range between 14% and 26% at the input power of 90–210 W. It should be pointed out that the uncertainty of the heat rates could be controlled by setting an appropriate flow rate range. It is also indicated in Fig. 9 that the uncertainty of the total heat rate predicted by measuring the heat losses is much smaller than that of Q_{top} and Q_{bot} estimated by using the calorimetry. That is the reason why the measurement of heat losses is used as the actual heat rate through the heat pipe.

All of the experimental data such as the temperatures, the input power and the coolant flow rates are acquired 50 times in an interval of 1 min and the average values on the 50 consecutive data are recorded after a steady state is reached. The use of the mean values is

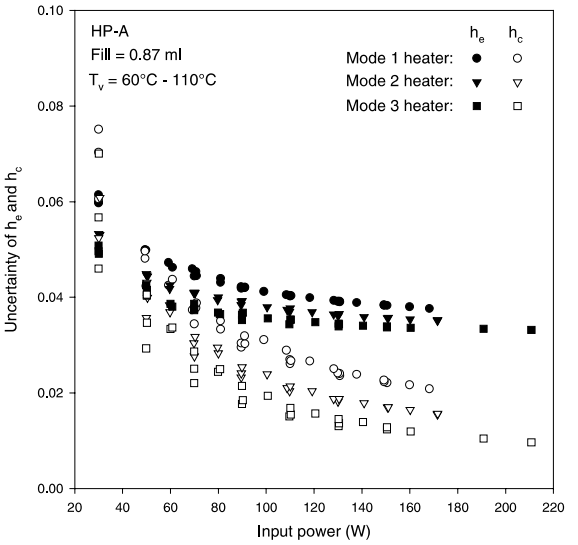

Fig. 10. Uncertainties of the heat transfer coefficients for HP-A in relation with the input power.

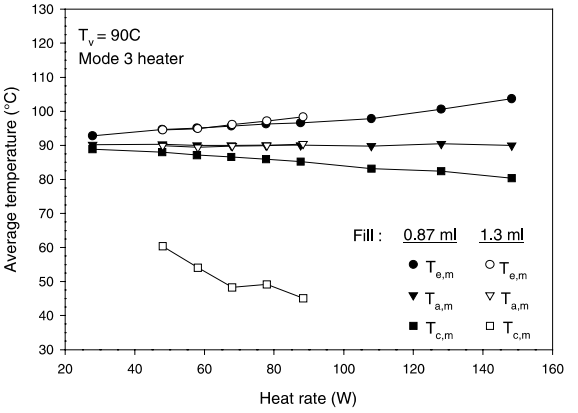

Fig. 11. Effect of fill amount on the average temperatures in the evaporator and condenser vs. the heat rate for HP-A with mode 3 heater.

appropriate to reduce the effect of the fluctuation of the tested parameters at high heat fluxes in the evaporator.

Overall uncertainties of the heat transfer coefficients of evaporator and condenser are estimated. For HP-A with 0.87 ml fill amount, the predicted overall uncertainties for h_e and h_c are shown in Fig. 10. The highest uncertainty for h_e and h_c occurs at the lowest input power. Given an input power, the uncertainties h_e and h_c are the highest for mode 1 heater and the lowest for mode 3 heater. This is because a different thermocouple number is used for each heating mode. The uncertainty decreases more noticeably for h_c than for h_e with an increase in the input power. The variation of uncertainties for different MHPs is less than 2% under the same operating conditions.

6. Thermal performance results and discussion

6.1. Preferable fill amounts

First of all, the thermal performance test for the heat pipes with various fill amounts is conducted for a few operating temperatures to determine appropriate fill amounts for the heat pipes with the two different types of capillary structures. Then, more experiments at various operating temperatures and heat rates are conducted using the preferable fill amounts for HP-A and HP-B and results for HP-A and HP-B are compared.

Fig. 11 shows the effect of working fluid fill amount on the average temperatures in the evaporator and condenser for HP-A with mode 3 heater. The operating temperature is 90 °C. It is evident that the average condenser temperature for the 1.3 ml fill amount is much lower than that for the 0.87 ml. The average evaporator-to-condenser temperature difference, $\Delta T_{ec}(\Delta T_{ec} = T_{e,m} - T_{c,m})$, is much smaller for the 0.87 ml than for the 1.3 ml. The reason is that the capillary fin in the condenser is submerged in the working fluid for the case of the 1.3 ml fill amount. The excess liquid above the fin tip results in a lower condensation heat transfer coefficient due to a lower thermal conductivity of the liquid. The fill amount of 0.87 ml is equivalent to a fill ratio of 80% that is defined by the ratio of the working fluid volume to the volume of all the grooves. Because of this result, the fill amount of 0.87 ml or one close to it is used for the capillary fin heat pipes.

6.2. Axial temperature profiles

Fig. 12(a), (b) and (c) show temperature profiles along the top and bottom surfaces of HP-A with the 0.87 ml fill amount at $T_v = 90$ °C for mode 1, mode 2 and mode 3 heating configurations. The input heat rate is varied from 60 to 250 W. In Fig. 12(a) for mode 1 heater, with an increase in the heat rate, the temperatures on the bottom of the evaporator increase and the temperatures in the condenser decrease. The peak temperature at the second thermocouple location where the chip resistor is active increases noticeably with increasing the heat rate. At 110 W, the temperature difference between the peak temperature and the operating temperature reaches 30 °C. In Fig. 12(b) for mode 2 heater, the evaporator temperatures on the top surface are slightly higher than those on the bottom and the condenser temperatures on the top surface are slightly lower than those on the bottom at the input power level of 60, 90 and 110 W. At 150 W, the peak temperature is greater on the bottom surface than on the top and the temperature difference between the peak temperature

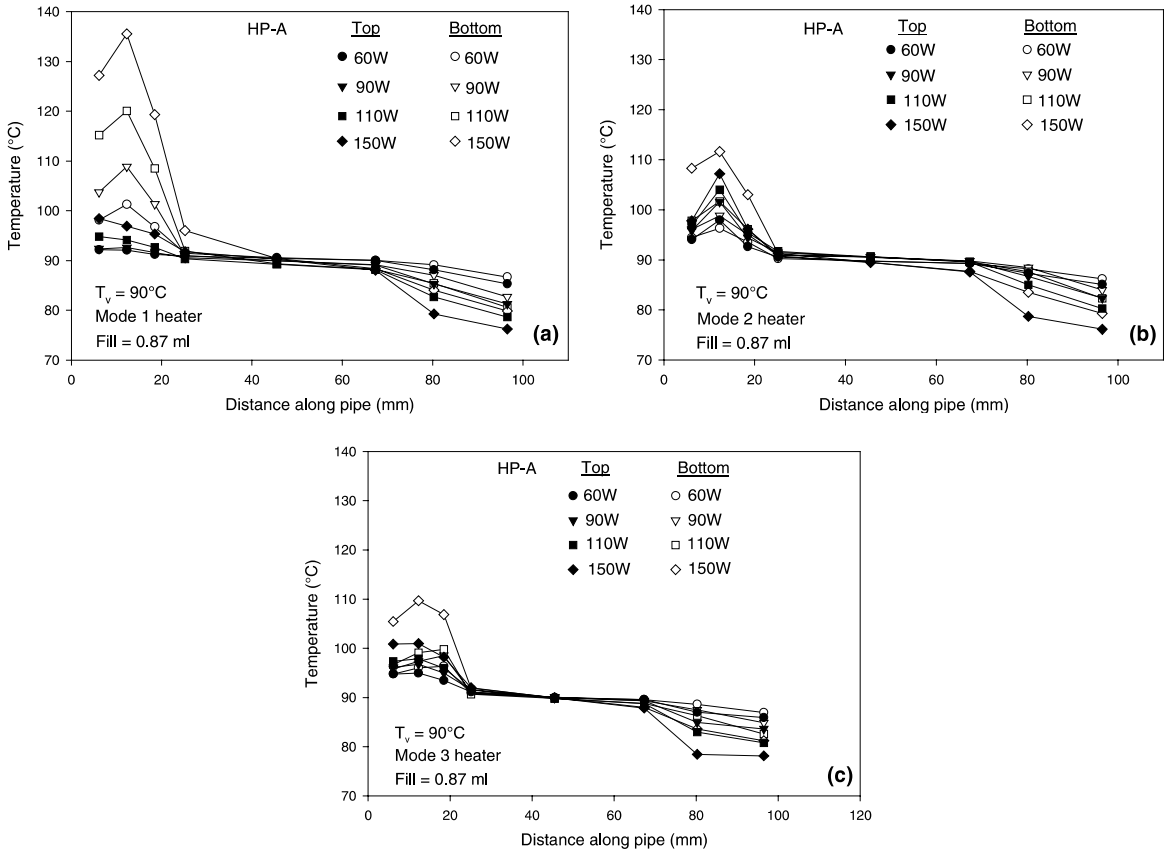

Fig. 12. Temperatures on the top and bottom surfaces of HP-A with 0.85 ml fill amount.

and the operating temperature is 22 °C. In Fig. 12(c) for mode 3 heater, the temperature profiles on the top surface are slightly different from those on the bottom at 60, 90 and 110 W. At 150 W, the temperatures on the bottom surface of the evaporator are noticeably higher than those on the top surface.

Fig. 13(a), (b) and (c) show temperature profiles along the top and bottom surfaces of HP-B for mode 1, mode 2 and mode 3 heating configurations. The working fluid fill amount is 0.85 ml. The operating temperature is 90 °C. In Fig. 13(a), with an increase in the heat rate, the temperatures on the bottom of the evaporator increase, more significantly than on the top, and the temperatures in the condenser decreases. The peak temperature is related to the place of the active chip resistor. At 110 W, the temperature difference between the peak temperature and the operating temperature reaches 30 °C similar to the case of HP-A (Fig. 12(a)). In Fig. 13(b) and (c), the evaporator temperatures on the top surface are slightly higher than those on the bottom and the condenser temperatures on the top surface are slightly lower than those on the bottom for the same input power level. In Fig. 13(c), the highest temperature along the heat pipe occurs at the first thermocouple location for the same input power level.

6.3. Effect of condenser cooling rate

Fig. 14 shows a ratio of the heat rate through the top cooler to that through the bottom cooler for HP-A with the 0.87 ml fill amount. The heat rate ratio is presented as function of the input power for the operating temperatures of 80 °C and 110 °C and for mode 2 and mode 3 heaters. In most cases, the heat rate ratios for mode 2 and mode 3 heaters are approximately the same for the same operating temperature. The operating temperature does have an effect on the heat rate ratio. In the case of mode 2 heater, the heat rate ratio decreases from 1.6 to 1.25 with the input power increased from 90 to 150 W at 80 °C and from 1.0 to 0.75 with the input power increased from 80 to 160 W at 110 °C. The heat rate ratio is greater at 80 °C than at 110 °C. This may be attributed to a coupled effect of the surface tension and gravity on the curvature of liquid–vapor interface.

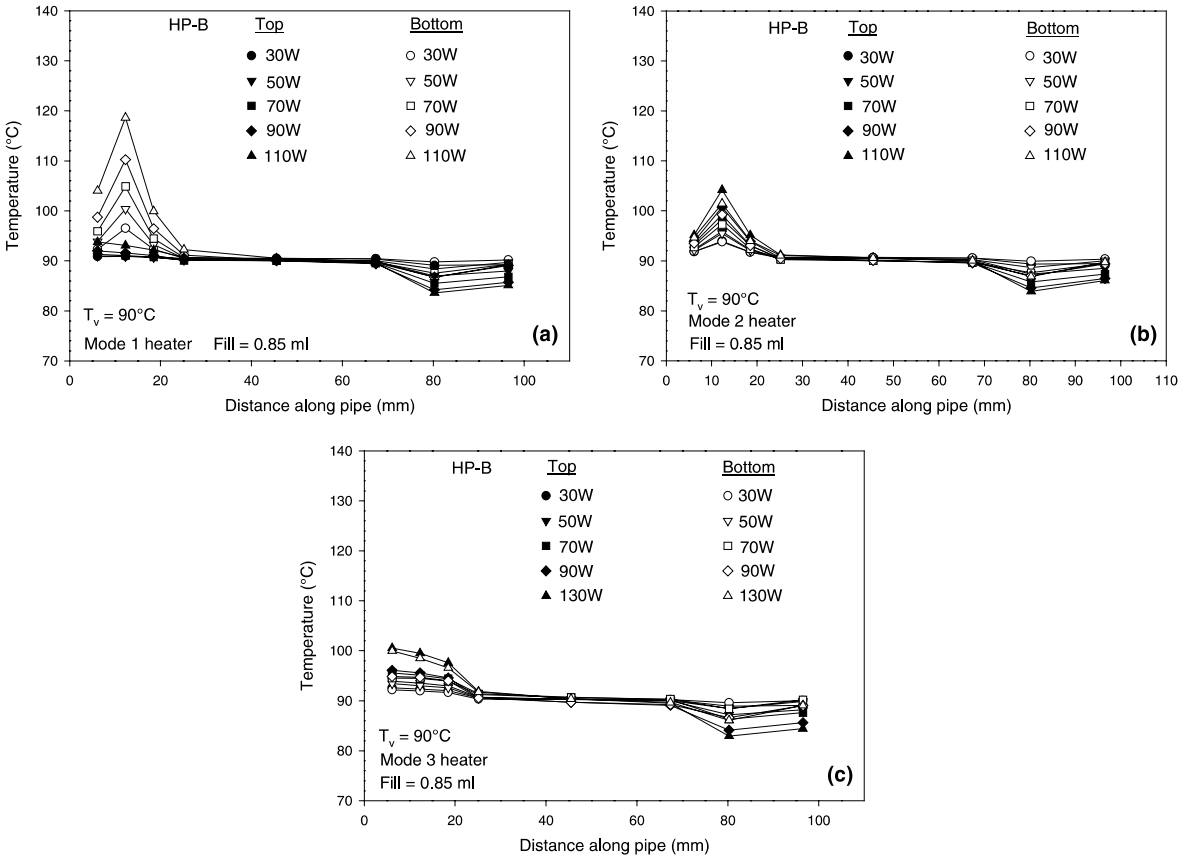

Fig. 13. Temperatures on the top and bottom surfaces of HP-B with 0.85 ml fill amount.

6.4. Comparison of thermal performances between HP-A and HP-B

To estimate the thermal performance of HP-A and HP-B, the evaporator and condenser heat transfer coefficients are defined as follows:

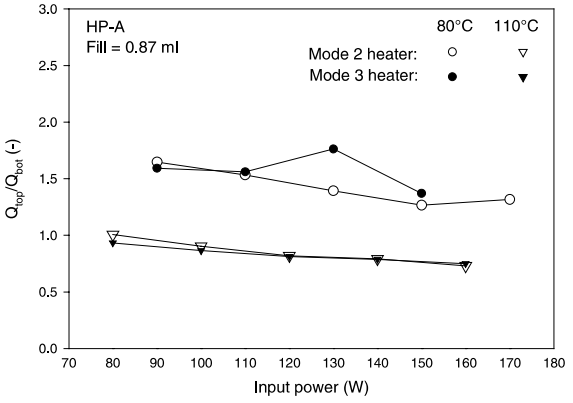

Fig. 14. Ratio of the heat rate through the top cooler to that through the bottom cooler for HP-A with 0.87 ml fill amount.

$$h_e = \frac{Q}{A_h(T_{e,i,m} - T_{a,m})}, \tag{2}$$

$$h_c = \frac{Q}{A_c(T_{a,m} - T_{c,i,m})}, \tag{3}$$

where the inner wall average temperatures of the evaporator and condenser are calculated as follows:

$$T_{e,i,m} = T_{e,m} - \frac{Qt_w}{A_h k_w}, \tag{4}$$

$$T_{c,i,m} = \frac{Qt_w}{A_c k_w} + T_{c,m}, \tag{5}$$

where Q is the heat rate, A_h the heating surface area dependent on the number of active chip resistor ($A_h = n_h A_1$), A_c the cooling surface area ($A_c = 2L_c B$), t_w the heat pipe wall thickness, and k_w is the thermal conductivity of the wall material (390 W/m K). The heat transfer coefficients depend on the type of capillary structure, the heat rate and operating temperature.

Fig. 15(a) shows the comparison of the heat transfer coefficient of evaporator between HP-B and HP-A at the operating temperatures of 60, 90 and 110 °C for mode 2

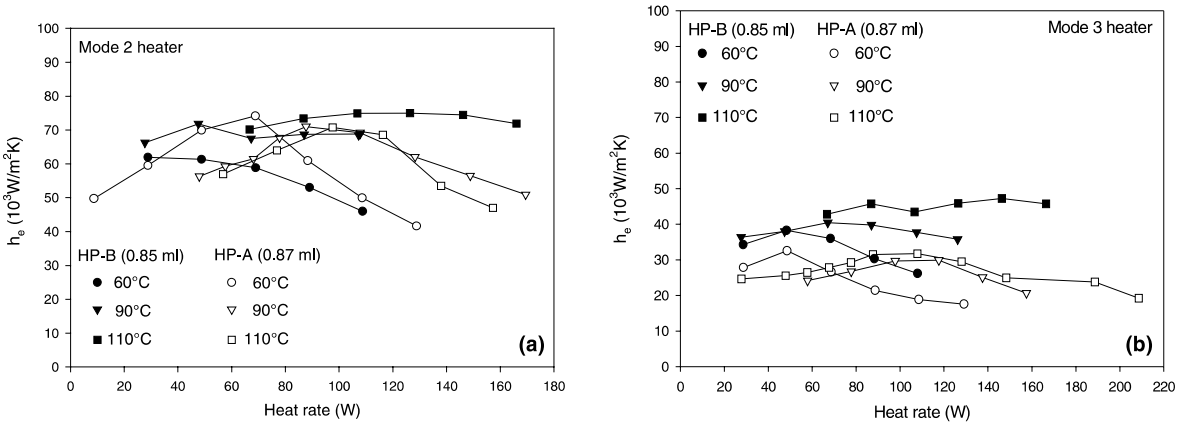

Fig. 15. Comparison of the heat transfer coefficient of evaporator between HP-B and HP-A.

heater. The profiles of h_e for HP-B do not have the noticeable crest while those for HP-A have it. The maximum values of h_e for HP-A do not vary much with the operating temperature and occurs at a higher heat rate if the operating temperature is increased. At 60 °C, most values of h_e are higher for HP-A than for HP-B. At 110 °C, the values of h_e are higher for HP-B than for HP-A. For the high heat rate, e.g., higher than 120 W, the value of h_e is or tends to be greater for HP-B than for HP-A. Fig. 15(b) shows the comparison of the heat transfer coefficient of evaporator between HP-A and HP-B for mode 3 heater. It is clear that the evaporator heat transfer coefficients are greater for HP-B than for HP-A for the same operating temperature of 60, 90 and 110 °C. In the range of the tested heat rate, the increase in h_e for HP-B is varied upward from 17% to 95% in comparison with HP-A. A larger increase occurring at operating temperature of 110 °C. Fig. 16(a) shows the comparison of the heat transfer coefficient of condenser between HP-A and HP-B at 60, 90 and 110 °C for mode 2 heater. It is evident that the condenser heat transfer coefficients are greater for HP-B than for HP-A. The heat transfer enhancement is more significant at 110 °C. The value of h_c for HP-B is increased by 123% or greater at 110 °C in comparison with HP-A. Fig. 16(b) shows the comparison of the heat transfer coefficient of condenser between HP-A and HP-B for mode 3 heater. Like the case with mode 2 heater, the condenser heat transfer coefficients are noticeably greater for HP-B than for HP-A. At 110 °C, the value of h_c is enhanced by 120% or greater. For HP-A, at heat rates greater than 28 W, the value of h_c decreases slightly with an increase in the heat rate. Given a heat rate, in most cases, an increase in the operating temperature results in a slight increase in h_c for HP-A and a noticeable increase for HP-B. Most condenser heat transfer coefficients for HP-A vary between 19 000 and 35 600 W/m^2 K while those for HP-B vary between 40 000 and 73 000 W/m^2 K.

The fin bridges (the uncut part) existing at the top of the folded sheet fin partially separate the liquid flow

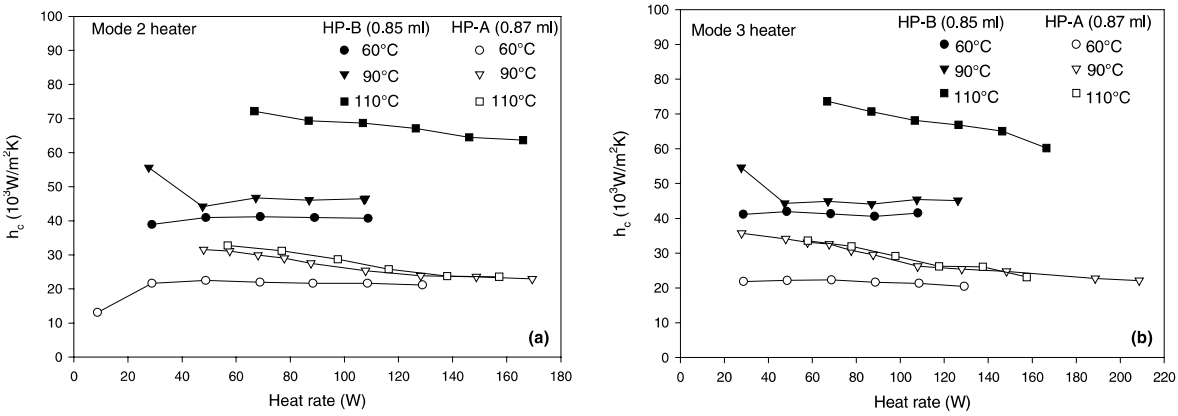

Fig. 16. Comparison of the heat transfer coefficient of condenser between HP-B and HP-A.

Table 2
Comparison of the average temperatures between HP-A and HP-B for mode 2 heater at high q_e

T_v (°C)		60	80	90	100	110
Q (W)		125	172	198	219	244
q_e (W/cm^2)		80.4	111	127	141	157
$T_{e,m}$ (°C)	HP-A (0.87 ml)	90.67	122.2	136.9	139.8	152.4
	HP-B (0.85 ml)	82.63	114.5	119.6	126.6	126.4
$T_{c,m}$ (°C)	HP-A (0.87 ml)	50.13	67.68	76.69	84.93	93.90
	HP-B (0.85 ml)	54.36	73.58	83.51	92.22	102.9
ΔT_{ec} (°C)	HP-A (0.87 ml)	40.54	54.53	60.24	54.83	58.51
	HP-B (0.85 ml)	28.27	40.95	36.09	34.4	23.52

from the vapor flow and reduce the average countercurrent flow shear stress at the liquid–vapor interface. To some extent, this helps the evaporator be sufficiently wetted by the liquid flowing back through the grooves. At the high heat rate, the fin bridges protect the return liquid against being torn from the capillary fin. The fin bridges in the condenser serve as additional secondary heat transfer surfaces and contribute to the enhancement of condensation heat transfer. As a result, HP-B is superior to HP-A in the thermal performance. At high temperatures, part of the condensate on the upper fin surface (on the top cooler side) may be drained down to the fin bridges forming a liquid retention region due to gravity. Meanwhile, liquid droplets under the liquid retention region come off the fin and fall onto the bottom surface. The rest of the condensate in the upper inverted grooves flows back to the upper evaporator by the capillary pumping head. With the condensate in part being drained off, a portion of the upper fin surface is exposed and the condensation heat transfer is improved. This explains why the use of the folded sheet fin with notch cuts brings about more significant enhancement of the condensation heat transfer in HP-B at the higher operating temperature such as 110 °C.

The heat pipe thermal performance at high heat fluxes greater than 100 W/cm^2 is investigated with mode 1 and mode 2 heaters. Table 2 shows the average temperatures in the evaporator ($T_{e,m}$) and condenser ($T_{c,m}$) of HP-B and HP-A with mode 2 heater. The operating temperature is varied from 60 to 110 °C. The average condenser temperatures are greater for HP-B than for HP-A at the same heat fluxes. This means that the condenser heat transfer coefficient is still greater for HP-B than for HP-A at the high heat fluxes. The average temperatures of the evaporator are smaller for HP-B than for HP-A, indicating that the evaporator heat transfer coefficient is higher for HP-B than for HP-A. It is a fact that the high heat flux brings about a larger ΔT_{ec}. The value of ΔT_{ec} decreases with an increase in the operating temperature. For HP-B, as an example, the value of ΔT_{ec} reaches 36.09 °C at the operating temperature of 90 °C and heat flux of 127 W/cm^2, and decreases to 34.4 °C at 100 °C, even at a higher heat flux of 141 W/cm^2.

Very high heat fluxes can be achieved using mode 1 heater. During the experiment with mode 1 heater, no temperature excursion on the evaporator wall has been found in the operating temperature range between 60 and 100 °C even if the heat flux is increased up to 283 W/cm^2 at 100 °C and to 158 W/cm^2 at 60 °C. This means that the heat pipe is still operating in the quasi-steady state. However, the peak evaporator temperature has reached 170.4 °C for $T_v = 100$ °C and 112.6 °C for $T_v = 60$ °C. Meanwhile, the average condenser temperature is 92.4 °C for $T_v = 100$ °C and 55.1 °C for $T_v = 60$ °C. Apparently, the heat pipe has lost its commonly addressed advantages due to the high temperature difference between its peak evaporator temperature and operating temperature though its maximum performance has not been encountered. This feature pertains to the spot heated heat pipe with a heating area as small as 0.774 cm^2. In this case, the temperature difference between the peak temperature and operating temperature is a more critical parameter to evaluate the performance of the heat pipe. The objective of developing high performance heat pipes is to reduce their internal thermal resistance at the high heat flux.

7. Conclusions

It is easy to make capillary grooves as narrow and deep as desired through the present fabrication techniques. The most efficient and promising capillary structure from the standpoint of heat transfer is the folded copper sheet fins with notches cut in the evaporator and condenser. Achievements of the present investigation are concluded as follows.

The fill amount of 0.87 ml (80% fill ratio) or 0.85 ml (78% fill ratio) results in a favorable thermal performance for HP-A and HP-B. HP-B with the 0.85 ml fill amount has exhibited the lowest evaporator-to-condenser temperature difference and consequently the lowest internal thermal resistance.

For HP-A, the condenser heat transfer coefficient, $h_{c,}$ decreases slightly with an increase in the heat rate in most cases. Given a heat rate, an increase in the

operating temperature results in a slight increase in h_c. Most condenser heat transfer coefficients vary between 19 000 and 35 600 W/m^2 K. In most cases, the evaporator heat transfer coefficient, h_e, has the maximum value for HP-A at a given operating temperature. The maximum value occurs at a higher heat rate with an increase in the operating temperature.

For HP-B, the maximum value of h_e is not noticeable for a given operating temperature. With mode 3 heater, the increase in h_e for HP-B is varied upward from 17% to 95% compared with the case of HP-A. Most condenser heat transfer coefficients for HP-B vary between 40 000 and 73 000 W/m^2 K, much higher than those of HP-A. The condensation heat transfer enhancement is more significant at 110 °C. The increase in h_c by 120% or greater for HP-B can be achieved at 110 °C in comparison with HP-A. In HP-B, the fin bridges (the uncut part) existing at the top of the folded sheet fin partially separate the liquid flow from the vapor flow and reduce the average countercurrent flow shear stress at the liquid–vapor interface. In addition, the fin bridges in the condenser serve as additional secondary heat transfer area. As a result, HP-B is superior to HP-A in the thermal performance.

The ratio of the heat rate through the top side cooler to that through the bottom side cooler of the condenser decreases with an increase of the input power.

The heat pipe thermal performance at high heat fluxes greater than 100 W/cm^2 is investigated with mode 1 and mode 2 heaters. It has been indicated that the heat transfer coefficients of the evaporator and condenser are still greater for HP-B than for HP-A at the high heat fluxes. Very high heat fluxes are achieved using mode 1 heater with heating area of 0.774 cm^2. During the experiment with the mode 1 heater, no temperature excursion on the evaporator wall of the heat pipe has been found in the operating temperature range between 60 and 100 °C even if the heat flux is increased up to 283 W/cm^2 at 100 °C and to 158 W/cm^2 at 60 °C. However, the peak evaporator temperature has reached 170.4 °C for $T_v = 100$ °C and 112.6 °C for $T_v = 60$ °C. Concerning this, the temperature difference between the peak temperature and operating temperature is regarded as a more critical parameter to evaluate the performance of the heat pipe with a small heating area. The price for the operation at the very high heat flux is a resultant large evaporator-to-condenser temperature difference across the heat pipe length.

Acknowledgements

This research was sponsored by the Propulsion Directorate of the Air Force Research Laboratory (AFRL), Wright-Patterson Air Force Base, Ohio and performed at the Power Division's Thermal Laboratory. The authors would like to acknowledge the effort of Mr. Richard Harris (UDRI) who diligently established the experimental setup and data acquisition system and made several engineering drawings. The authors would also like to thank Roger Carr (UES) for helping with reducing data and John Tennant (UES) and Donald Reinmuller (AFRL) for their support in fabrication of the miniature heat pipes.

References

[1] T. Katoh, K. Amako, H. Akachi, New heat conductor for avionics cooling, in: 11th International Heat Pipe Conference, Tokyo, 1999.
[2] G.P. Peterson, An Introduction to Heat Pipes, Wiley, New York, 1994.
[3] A. Faghri, Heat Pipe Science and Technology, Taylor & Francis, London, 1995.
[4] F. Polasek, M. Zelko, Thermal control of electronic components by heat pipes and thermosyphons, in: 10th International Heat Pipe Conference, Stuttgart, 1997.
[5] D. Plesch, W. Bier, D. Seidel, K. Schubert, Miniature heat pipes for heat removal from microelectronic circuits, in: ASME Annual Meeting, Altanta, 1991.
[6] Y. Cao, M. Gao, J.E. Beam, B. Donovan, Experiments and analyses of flat miniature heat pipes, in: 31th Intersociety Energy Conversion Engineering Conference, Washington, DC, 1996.
[7] A. Faghri, D. Khrustalev, Micro/miniature heat pipe technology for electronic cooling, WL-TR-97-2083, Final Report, Wright Laboratory, AFMC, WPAFB, 1997.
[8] R. Ponnappan, A novel micro-capillary groove-wick miniature heat pipe, AIAA 2000-2947, 35th Intersociety Energy Conversion Engineering Conference, Las Vegas, 2000.
[9] M. Groll, S. Roesler, L. Lin, Investigation of vertical high-performance closed two-phase thermosyphons with perforated tube flow separators, in: International Symposium on Phase Change Heat Transfer, Chongqing, P.R. China, 1988.
[10] M.G. Grote, J.A. Stark, E.C. Tefft, Enhanced evaporative surface for two-phase mounting plates, in: 16th ICES Conference, Paper No. 860979, 1986.
[11] S.J. Kline, F.A. McClintock, Describing uncertainties in single-sample experiments, Mech. Eng., ASME (January) (1953) 3–8.